Article

Experimental Study Regarding the Possibility of Blocking the Diffusion of Sulfur at Casting-Mold Interface in Ductile Iron Castings

Denisa Anca, Iuliana Stan *, Mihai Chisamera, Iulian Riposan and Stelian Stan

Materials Science and Engineering Faculty, Politehnica University of Bucharest, 313 Spl. Independentei, 060042 Bucharest, Romania; denisa_elena.anca@upb.ro (D.A.); chisameramihai@gmail.com (M.C.); iulian.riposan@upb.ro (I.R.); constantin.stan@upb.ro (S.S.)

* Correspondence: iuliana.stan@upb.ro

Abstract: The main objective of this work is to investigate the mechanism of sulfur diffusion from the mold (sand resin P-toluol sulfonic acid mold, sulfur-containing acid) in liquid cast iron in order to limit the graphite degeneration in the surface layer of iron castings. A pyramid trunk with square section samples was cast. On the opposite side of the feed canal of the samples, steel sheets with different thicknesses (0.5, 1, and 3 mm) were inserted with the intention of blocking the diffusion of sulfur from the mold into the cast sample during solidification. The structure evaluation (graphite and matrix) in the surface layer and the casting body was recorded. The experimental results revealed that by blocking the direct diffusion of sulfur at the mold-casting interface, a decrease of the demodified layer thickness (for 0.5 mm steel sheet thickness) is obtained until its disappearance (for steel sheet thicknesses of more than 1 mm). The paper contains data that may be useful in elucidating the mechanism of graphite degeneration in the superficial layer of ductile iron castings. Based on the obtained results, we recommend using such barriers on the metal-mold interface, which are able to limit sulfur diffusion from the mold/core materials into the iron castings, in order to limit or even cease graphite degeneration in the Mg-treated surface iron casting layer. The paper presents additional data related to the interaction of sulfur at the ductile iron casting-mold interface previously analyzed.

Keywords: ductile cast iron; sulfur diffusion; structure; graphite degeneration; surface layer

1. Introduction

Although the graphite degeneration phenomenon was highlighted in the first iron castings, with compact graphite shapes obtained, not enough is known about the phenomenon at present. Many papers have identified its surface degenerated structure as an effect of sulfur diffusion from the mold into the Mg-treated iron melt [1–8].

The analysis of the demodifying graphite structure in the superficial layer of compact graphite iron castings requires the most accurate knowledge of physico-chemical processes at the liquid metal-mold interface. It is important especially in the cooling phase of liquid metal when it is in direct contact with the mold. During solidification, contact between the liquid and the mold is made by means of a solidified crust, which implies a slower diffusion and an interruption of the contact of the alloy with the atmosphere of the mold.

Previous works [1,6–10] have pointed out that decreasing the residual magnesium content aggravates the surface graphite degeneration five times more in mold including sulfur, compared with no-sulfur mold media. If the sulfur contribution of the mold is diminished, such as by blocking its transfer to the iron melt, the graphite degeneration in the casting surface layer can be avoided or, at least, diminished. Graphite degeneration in

the casting surface layer is promoted by a S-bearing coating, or conversely, it is possible to limit the surface layer thickness using desulfurization type coatings (Al_2O_3, $CaCO_3$, Basic slag, CaF_2, Talc, Mg), with Mg-bearing coatings as performance [1,6–8]. It has also been found that the negative role of oxygen and especially of sulfur in graphite degeneration in the surface casting layer can be counteracted by the addition of materials able to block the diffusion of these elements into the iron melt, such as carbonic material (more efficient to limit oxygen effect) and iron powder (especially to limit sulfur negative effects) [9].

Recently, it was found that in the presence of a thin steel sheet at the metal-mold interface, the thickness of the surface layer decreases or is just avoided. It was suggested that it acts as a barrier, blocking sulfur diffusion into the iron melt [10]. The present paper aims to elucidate some aspects of the demodifiyng process related to the mechanism of the transition of sulfur from the mold into liquid cast iron through the prism of the diffusion blocking effect at the interface.

2. Materials and Methods

The base iron melt was prepared using the induction furnace with acid liner (100 kg capacity, 2400 Hz frequency, Inductro, Bucharest, Romania). A total of 100 wt.% cast iron scrap, carbonic material (0.37 wt.% addition, >98 wt.% C) and CaC_2 (0.43 wt.% addition) were used as charge materials, and 2 wt.% FeSiCaMgRE (6 wt.% Mg) alloy was used as nodulizer (Tundish Cover treatment technique, Politehnica University, Bucharest, Romania), followed by ladle inoculation (CaBaFeSi, 0.5 wt.% addition). The thermal regime of iron melt processing was as follows: superheating temperature: T_s = 1550 °C; Mg-treatment temperature: T_m = 1530 °C; pouring temperature: T_p = 1350 °C. The inoculated Mg-treated iron was poured in a pyramid trunk with square section samples and with steel sheets (0.5, 1, and 3 mm thickness) inserted at the casting-mold interface (Figure 1). For comparison, a sample without a steel sheet was cast (for more details, see paper [10]).

The structure evaluation in the surface layer and the casting body was made according to Figure 2. Graphite morphology analysis [10] was conducted by using a professional automat image analyzer (OMNIMET ENTERPRISE and analySIS® FIVE Digital Imaging Solutions software version 5.0, Waukegan, IL, USA), using both the standard cast iron modulus and particle analysis software.
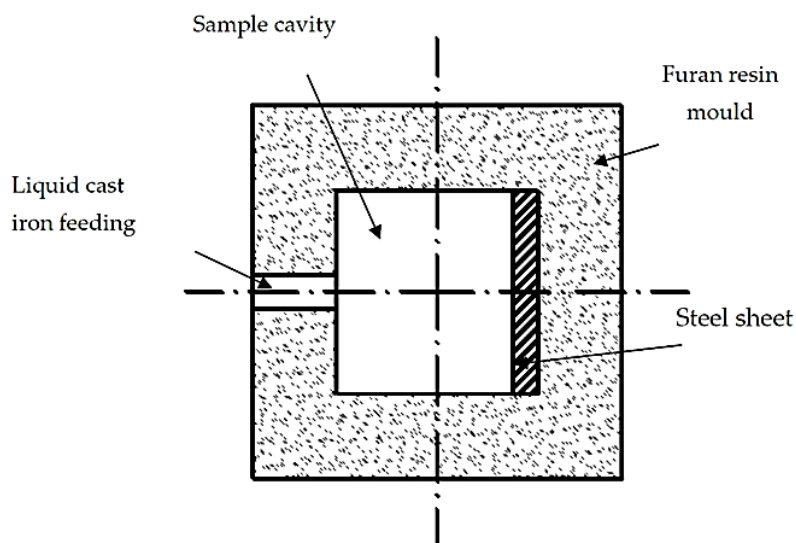

Figure 1. The inserted steel sheet position in mold (transversal section).
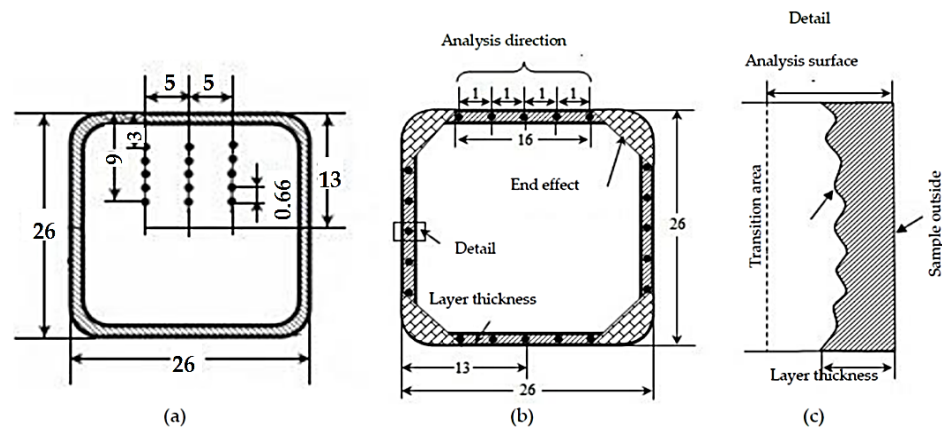
Figure 2. The analysis procedure to evaluate the structure parameters (graphite and metal matrix) in the casting body (**a**) and in the surface layer and skin (surface layer) thickness (**b,c**) (Units-mm).

The structure analysis in the casting body was recorded on the three parallel directions on a 5 mm casting thickness, starting at a 3 mm distance from the casting surface (Figure 2a). Nine analysis points, with a 0.66 mm distance between them in each direction, were used. The average value of the 27 analyses was considered.

Figure 2b,c shows the procedure of structure analysis on the section of the surface layer. In order to avoid the end effect, the structure analysis was recorded at a distance of 16 mm, with 17 analysis points each at a 1mm distance between them. The degenerated graphite layer was measured by metallographic microscope analysis (100:1 magnification) as a visible layer thickness up to prevalent nodular graphite morphology presence, in un-etched and Nital etched conditions. For this purpose, with the assistance of the automatic image analyzer, images of the degenerate layer were captured on the un-etched and Nital etched samples, on which measurements of the thickness of the degenerate layer were made, after the previous calibration of the instrument. The degenerate surface layer was delimited based on the visible decrease of graphite compactness, on the un-etched samples, and by measuring the thickness of the predominantly ferritic area determined by the decrease of graphite compactness. There are some differences between the two measurement variants because in the un-etched state the degenerate layer was more difficult to delimit, while the boundary pearlite/ferrite had a more visible contrast. The measurement points' layer thickness are at 100 μm between these points, with an average value consideration. Graphite nodularity (according to the relation (1)) on the casting section, starting from the casting surface, is also used to evaluate the skin thickness.

3. Results and Discussion

3.1. Chemical Composition

The chemical composition was evaluated for the base cast iron (wt.%: 3.37 C, 1.42 Si, 0.54 Mn, 0.021 S, 3.83 CE (carbon equivalent)), for the cast iron after the Mg-treatment (wt.%: 3.44 C, 2.56 Si, 0.62 Mn, 0.013 S, 0.059 Mg, 0.02 Ce, 0.0086 La, 4.24 CE), and inoculation (wt.%: 3.37 C, 2.93 Si, 0.62 Mn, 0.015 S, 0.048 Mg, 0.015 Ce, 0.006 La, 4.2 CE). The resulting ouble treated cast irons (Mg-treatment + Inoculation) are characterized by an eutectic position in the Fe-C diagram and a good nodulizing potential (Mg-Ce-La residual contents). The residual elements content is below the limits considered critical for the shape of graphite (wt.%: 0.006–0.012 Al, 0.005–0.006 Ti, 0.045–0.05 Cr, 0.036–0.037 Ni, 0.04–0.05 Cu, 0.008–0.009 Mo, 0.005–0.006 Co, 0.002–0.003 V, 0.0002–0.0004 Pb, 0.0004–0.0005 Sn, 0.0055–0.006 As, <0.001 Sb, <0.001 Te, 0.0009–001 B, 0.0002–0.0005 Zn, 0.008–0.01 N, <0.0005 Bi).

3.2. Structure Characteristics

Nodular graphite morphology characterizes the structure of the casting body, with more than 80% graphite nodularity (Equation (1) in all of the tested variants (Figure 3)).

$$N = [(\sum A_{NG} + 1/2\sum A_{IG})/\sum A_{tot}] \times 100\% \tag{1}$$

where

A_{NG}—area of particles classified as nodules (RSF = 0.625–1.0);

A_{IG}—area of particles classified as intermediates (RSF = 0.525–0.625);

A_{tot}—area of all of the graphite particles;

RSF—roundness shape factor = $4A/\pi l^2$;
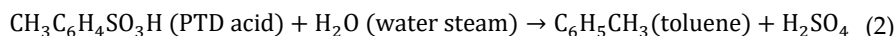
A—area of the graphite particle in question;

l—maximum axis length of the graphite particle in question (maximum distance between two points on the graphite particle perimeter).

The presence of the steel sheet at the mold–cavity interface led to graphite nodularity improvement (5%) and the nodule count increasing (1.5 time), with the presence of the fine nodules (max. 30 μm, Size 7, ISO 945) 1.75 time higher, favoring the ferrite amount increasing in the casting body. Under steel sheet influence, acting as a chilling agent (higher cooling rate), a limited amount of carbides resulted (2%–4%).
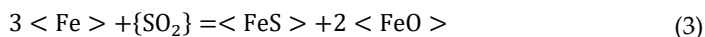
By blocking direct diffusion at the interface with the help of steel plates, a decrease in the thickness of the demodified layer (0.5 mm sheet thickness) was obtained until its disappearance (at 1 and 3 mm sheet thicknesses) (Figure 4).

At 0.5 mm sheet thickness, a discontinuous layer of degenerate graphite appeared. Its appearance may have been due to the rapid overheating of the steel sheet and the layer's arrival in a semi-viscous state, which favored the diffusion of sulfur from the mold in liquid cast iron. It was found that the layer thicknesses obtained on the samples etched with Nital 2% were higher than those obtained by measuring on un-etching samples, which confirms that the demodifying effect is manifested inside the samples, inducing changes in the metal matrix.

It is suggested that in the first stage of solidification, the diffusion of sulfur from the furan resin mold in steel sheet occurred. By pouring the iron melt into the furan resin mold, under the water vapors and the temperature action, P-toluol sulfonic acid (PTS) dissociated with sulfuric acid forming, according to the Equation (2):

$$CH_3C_6H_4SO_3H \text{ (PTD acid)} + H_2O \text{ (water steam)} \rightarrow C_6H_5CH_3 \text{(toluene)} + H_2SO_4 \tag{2}$$

The dissociation of sulfuric acid and aromatic sulfonic acids from the catalyst composition (which ensures furan resin ionic polymerization and the mold hardening) resulted in the SO_2 migrating to the interface and creating a concentration of sulfur on the metal surface following the Equation (3):

$$3 < Fe > + \{SO_2\} = < FeS > +2 < FeO > \tag{3}$$

The reaction was similar to the sulfurizing process of the solid metal charge in the cupola of gaseous atmospheres containing SO_2.
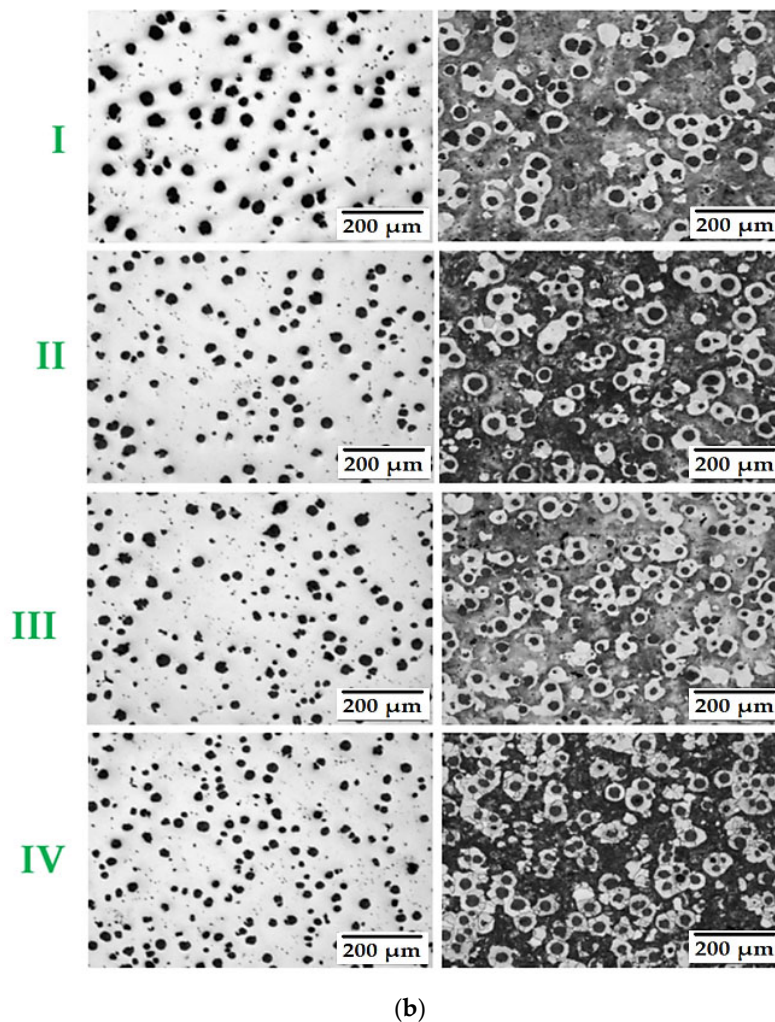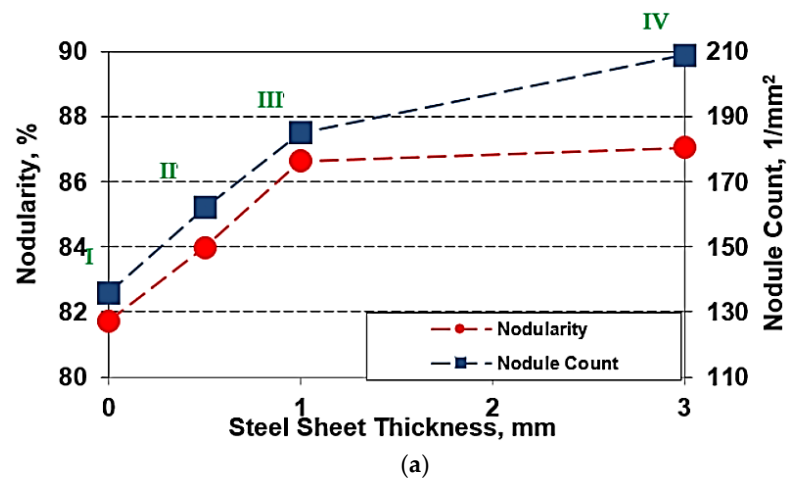
(**a**)

(**b**)

Figure 3. Graphite Nodularity and Nodule Count (**a**) and Structure (**b**) in the casting body as steel sheet thickness influence in un-etching and etching conditions, respectively (**I**-sample without steel sheet, **II**-sample with 0.5 mm steel sheet thickness, **III**-sample with 1 mm steel sheet thickness, **IV**-sample with 3 mm steel sheet thickness).
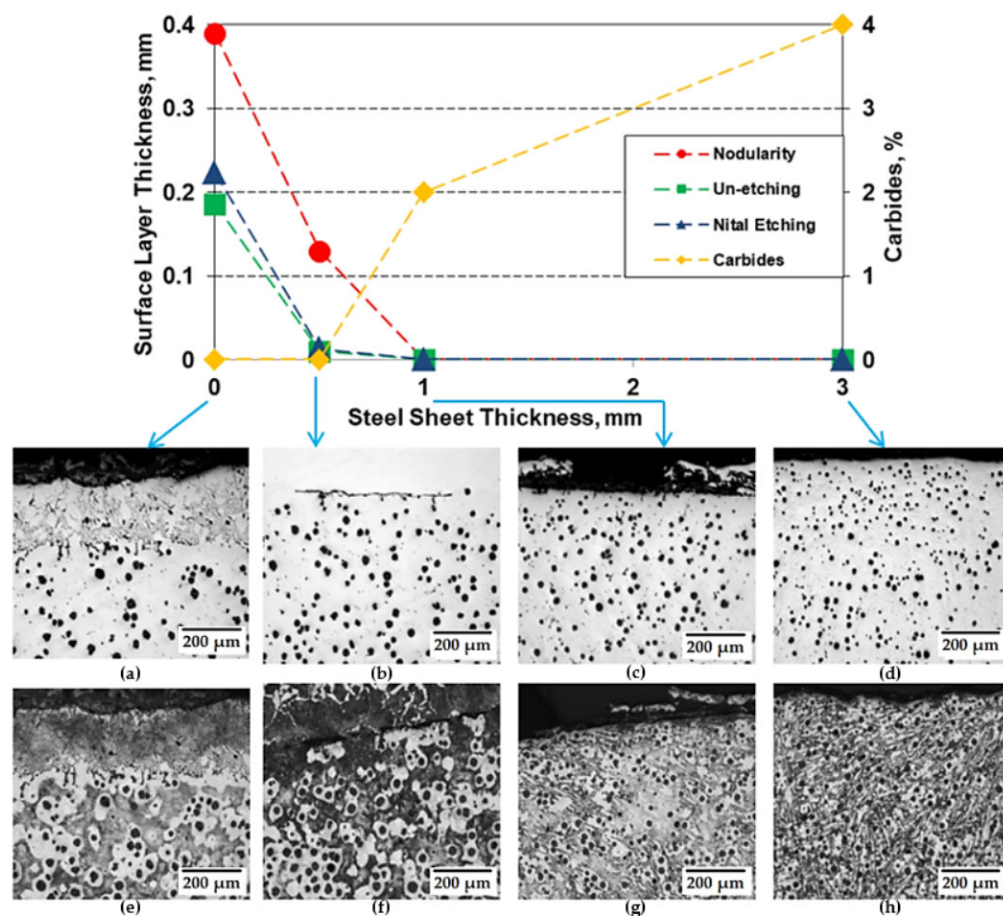
Figure 4. Graphite degenerated layer thickness as steel sheet thickness influence in un-etching and Nital etching conditions, respectively. Superficial layer structure as reference (**a**,**e**), 0.5 mm steel sheet influence (**b**,**f**), 1 mm steel sheet influence (**c**,**g**) and 3 mm steel sheet influence respectively; **a**, **b**, **c**, **d**-un-etched samples; **e**, **f**, **g**, **h**-Nital etched samples.

From the ΔG relation ($\Delta G = -73500 + 25.33T$, J), it resulted that with the temperature increase, the reaction was carried out to the left, in the sense of sulfur oxidation. However, experiments [11] performed by maintaining a sample of steel in the SO_2 atmosphere have shown that as the temperature increases the sulfurization process intensifies, especially above the temperature of 800 °C [12]. This has been attributed to the formation of sulfur eutectics that pass into the liquid state (FeO-FeS, at 940 °C and Fe-FeS, at 975 °C), favouring the adsorption of sulfur from gases. At the same time, the temperature increase determines the diffusion intensification process of sulfur through the solid metal, reducing its concentration in the superficial area, thus favoring the reaction to the right.

The formed iron sulfide determined the concentration of sulfur in the superficial layer of the steel sheet and created the conditions for diffusion through the steel sheet in which the concentration of sulfur was lower (less than 0.05 wt.% S).

In the second stage, the diffusion of sulfur from the steel sheet in the liquid cast iron sample occurred.

In the case of steel sheet barriers introduction, the time of solid crust formation was considerably reduced due to an increase of the solidification constant.

In the first stage, the diffusion of sulfur from the furan resin mold and the steel sheet occurred.

The diffusion of sulfur from the gas phase through the steel sheet is governed by Fick's second law, whose analytically transposed solution for flat finite media and short durations is:

$$F = \frac{C_m - C_0}{C_s - C_0} = 1.128 \times \frac{\sqrt{D \times t}}{l} \qquad (4)$$

where

F is the sulfur saturation fraction;

C_m—the average concentration of the broadcast substance (in our case, sulfur) at time t > 0;

C_0—the initial concentration of the broadcast substance at time t = 0 (in our case, the sulfur concentration in the steel sheet, S_0 = 0.05%–0.06%) is admitted: S_0 = 0.055 wt.%;

C_s—the concentration of the broadcast substance at the interface (the sulfur content in the boundary layer created by the reaction between Fe and SO_2); for the calculation, the sulfur concentration at the interface is considered 1 wt.%;

D—the diffusion coefficient of sulfur in the solid steel sheet (at a temperature of 1000 °C, D_s = (2...7) × 10^{-10} cm²/s [11]);

l—the distance on the sheet depth.

For a steel sheet with 0.5 mm thickness, at t = 10 s, it results:

$$F = \frac{1.128\sqrt{4.5 \cdot 10^{-10} \cdot 10}}{0.5 \cdot 10^{-1}} \simeq 0.0015$$

Result:

$$\frac{C_m - C_0}{C_s - C_0} = \frac{C_m - 0.055}{1 - 0.055} = 0.0015$$

C_m = 0.0564 wt.%, which means an increase of sulfur in the steel sheet of about 2.6 wt.% after 10 s.

For steel sheets of 1 mm and 3 mm, respectively, the concentrations C_m = 0.0550 wt.% S result, which means that at thicknesses greater than 1 mm there is no noticeable concentration of sulfur in the sheets (C_m = C_0).

Next, the diffusion of sulfur from the steel sheet into the liquid cast iron from the sample:

- The diffusion coefficient of sulfur in liquid cast iron at 1400 °C is [11]: D_s^{1400} = 3.50 × 10^{-5} cm²/s;
- The sulfur concentration in the steel sheet after the diffusion of sulfur from the mold, C_s = 0.0564 wt.% (calculated);
- Sulfur concentration in modified cast iron, C_0 = 0.015 wt.%;
- Diffusion layer thickness is considered equal to the demodified layer average thickness (for the present example, on the 0.5 mm steel sheet, a demodified layer determined by means of the shape factors, δ_{str} = 0.13 mm, resulted [10]);

The sulfur saturation fraction according to Equation (4) is:

$$F = \frac{1.128\sqrt{3.5 \times 10^{-5} \times t}}{0.13 \times 10^{-1}} = 0.51 \times \sqrt{t} = \frac{C_m - C_0}{C_s - C_0} = \frac{C_m - 0.015}{0.0564 - 0.015}$$

The average concentration of sulfur in the broadcast layer results,

$$C_m = 0.015 + 0.0211 \times \sqrt{t} \qquad (5)$$

Example: For t = 10 s, C_m = 0.0817 wt.% S.

This amount of sulfur can annihilate 0.0817 · 24/32 = 0.061 wt.% Mg; thus, more than the residual Mg content of cast iron (0.048 wt.%). This explains the appearance of a small degenerated layer in the sample.

The diffusion of sulfur in liquid cast iron was limited by the solidified cast iron crust formation at which the diffusion coefficient is much lower (D_s = (2...7) × 10^{-10} cm²/s, at a temperature of 1000 °C) [11]. In this context, it would have been useful to determine the moment of solid crust formation at the interface.

For the samples analyzed in this paper, a law of solidified crust thickness variation (δ) resulted like: $\delta = 0.908 \times 10^{-3} \times \sqrt{t} = 3.12 \times 10^{-3}$ m whence it results for $\delta = 0$, $\sqrt{t} \geq \frac{3.12}{0.908} \geq 11.8$ s.

This means that after about 12 s from the casting, the solid crust formation began for the samples cast in the furan resin mold, without steel sheets.

During this time, reactions at the interface between the liquid iron during cooling and the mold developed.

In the case of the steel sheet barriers' introduction, the solid crust formation duration was considerably reduced due to the increase of the solidification constant. For example, at an estimated value of the solidification constant in the case of casting in steel molds, k = 2.8×10^{-3} m/s$^{1/2}$, a duration of solidified crust formation of about 1.2 s results. This is also the reason why the demodified layer thickness in the ductile cast iron samples, in which steel sheets at the interface were inserted, was practically zero compared to the sample without protection sheets in which the demodified layer thickness exceeded 200 µm. Moreover, as resulted from the calculations, at steel sheet thicknesses greater than 1 mm, this became an effective barrier against the diffusion of sulfur from the mold into the cast piece.

Besides the main effect of degeneration of the graphite, other effects of sulfur diffusion were recorded, considered secondary but with implications on the quality of the surface layer:

- The chill effect (free carbides formation) occurred in the white cast iron layer formation (ledeburite + cementite + pearlite) in the interface areas where liquid cast iron infiltrated into the pores of the mold (Figure 5a,b). In these areas, due to the large contact surface between the liquid iron and the mold, the diffusion of sulfur was favoured, leading to concentrations of over 0.3 wt.%–0.4 wt.% S at which its free carbides formation effect was visible. This is only a supposition. Future investigation must elucidate this aspect.

- Formation of complex compounds in the surface layer of the samples and in the slag film on their surface (Figure 5c,d). They were evaluated only by morphologic aspect. Energy-dispersive X-ray analysis (EDAX)examinations are needed for quantification.

- Formation of graphite particles with an advanced degree of degeneration, indicating changes in growth directions and Mg/S ratio as a result of changes in sulfur concentration (Figure 5e).

The steel sheets could not be fully melted due to their high melting temperature, but they created effects at the interface due to the diffusion of carbon from cast iron into steel, increasing the cooling rate of liquid cast iron at the interface and limiting the transition of sulfur from mold to cast iron due to the much lower diffusion rate in the solid state compared to the liquid state. These effects were manifested by:

- Formation of mixed graphite structures at the interface (Figure 6a);

- Modification of the matrix structure in steel sheets from ferritic to ferrite-pearlitic and even hypereutectoid steel (pearlite + secondary cementite), due to the strong diffusion of carbon from the liquid cast iron into the steel sheets (Figure 6b);

- Formation of metastable cast iron structures (pearlite + cementite + graphite) (Figure 6c).

These effects, visible in the steel sheet with a thickness of 0.5 mm, faded in those with greater thicknesses (1–3 mm), where it took the cooling effect to slow down the diffusion processes, and these effects favored the rapid formation of a solid cast iron crust in which the demodification effect no longer manifested.
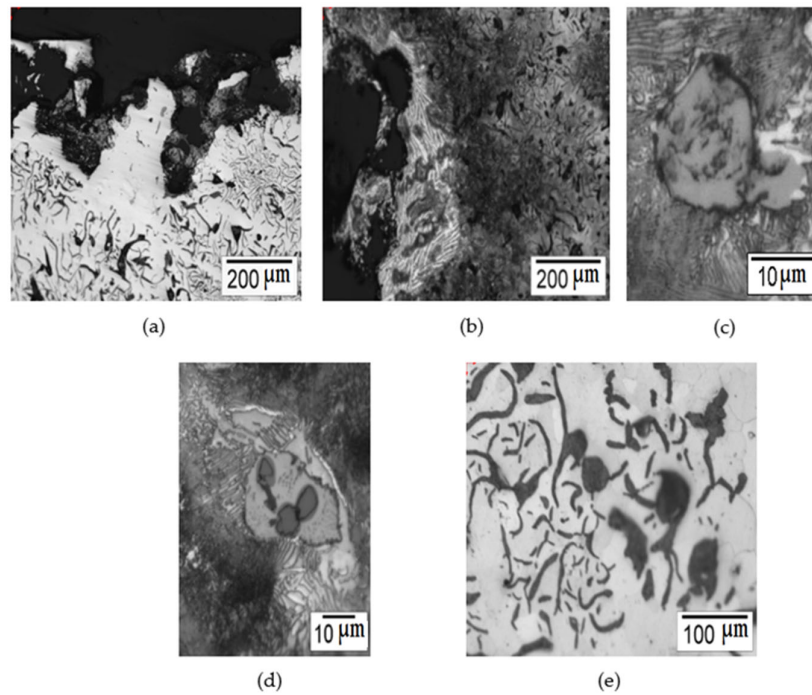
Figure 5. Effects of sulfur in the surface layer of cast samples: (**a**,**b**)-free carbides formation; (**c**,**d**)-formation of complex compounds; (**e**)-complex graphite shapes.
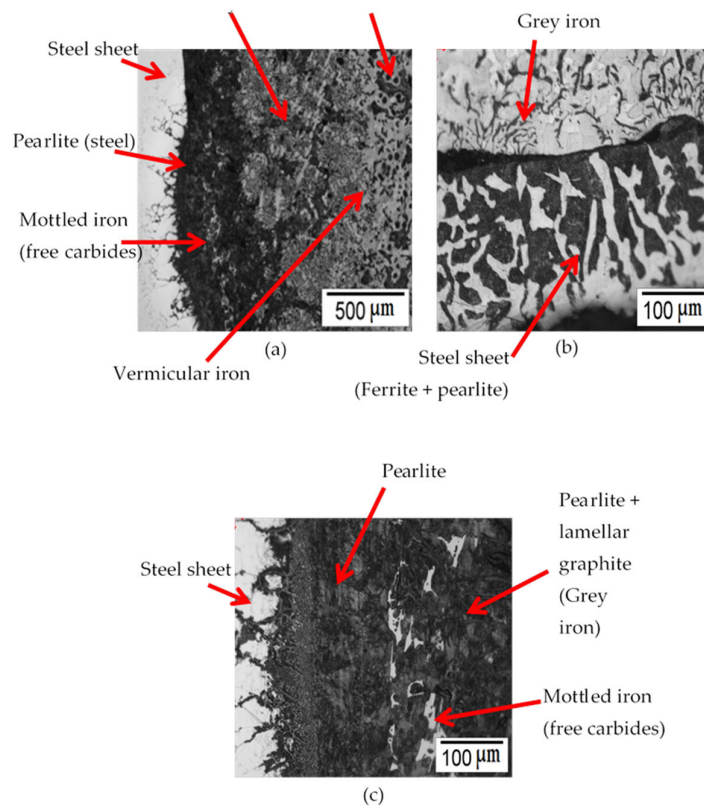

Figure 6. The steel sheets' effects on the interface liquid ductile iron-furan resin mold: (**a**)-mixed structures at the interface (steel-cast iron); (**b**)-Widmannstaten structure in the steel sheet; (**c**)-mottled cast iron structure in the surface layer (details from photo (**a**)).

4. Conclusions

The introduction of barriers to the liquid cast iron-mold interface, in the form of steel sheets, has generated effects depending on their ability to change the thermal balance of solidification.

In the case of using steel sheets with a 0.5 mm thickness, the presence of degenerate graphite was observed in the surface layer, which means that there was a diffusion of sulfur.

The steel sheet with a 0.5 mm thickness, although not completely assimilated, did not eliminate the effect of superficial demodification, but caused secondary effects due to a change in the thermal balance at the interface, given that the diffusion processes, especially of C and S, generated the formation of complex structures specific to cast iron–steel border areas.

The steel sheets with 1–3 mm thickness also stopped the superficial demodification process, by accelerating surface cooling and favoring the early formation of a solidified cast iron crust in which the demodification effect does not occur. It can be said that at higher thicknesses, the steel sheets show the effect of external coolers. The role of coolers is highlighted by the finishing of graphite in cast iron samples and the appearance of carbides in the metal matrix.

Theoretical calculus shows the possibility of sulfur diffusion limitations by the use of protective steel sheets in the liquid-mold interface. The thickness of these sheets must be calculated as dependent on casting solidification parameters (casting modulus, purring temperature, eutecticity degree of ductile iron, etc.). Future investigations are necessary in order to establish the concrete conditions of practical applications.

References

1. Ivan, N.; Chisamera, M.; Riposan, I. Influence of magnesium content and coating type on graphite degeneration in surface layer of iron castings in resin sand—PTSA molds. *ISIJ Int*. **2012**, *52*, 1848–1855.
2. Boonmee, S.; Stefanescu, D.M. Occurrence and effect of casting skin in compacted graphite iron. *Int. J. Cast. Met. Res*. **2016**, *29*, 47–54.
3. Stefanescu, D.M.; Wills, S.; Massone, J.; Duncan, F. Quantification of casting skin in ductile and compacted graphite irons and its effect on tensile properties. *Int. J. Met*. **2008**, *2*, 7–28.
4. Labrecque, C.; Gagne, M.; Cabanne, P.; Francois, C.; Beret, C.; Hoffmann, F. Comparative study of fatigue endurance limit for 4 and 6 mm thin wall ductile iron castings. *Int. J. Met*. **2008**, *2*, 7–17.
5. Danko, R.; Gorny, M.; Holtzer, M.; Zymankowska-Kumon, S. Effect of the quality of furan molding sand on the skin layer of ductile iron castings. *ISIJ Int*. **2015**, *54*, 1288–1293.
6. Chisamera, M.; Ivan, N.; Riposan, I.; Stan, S. Iron casting skin management in no-bake mold—Effects of magnesium residual level and mold coating. *China Foundry* **2015**, *12*, 222–230.
7. Ivan, N.; Chisamera, M.; Riposan, I.; Stan, S. Control of graphite degeneration in the surface layer of Mg-treated iron castings in resin sand—P-Toluol Sulphonic Acid (PTSA) molds. *AFS Trans*. **2013**, *121*, 379–390.
8. Anca, D.; Chisamera M.; Stan, S.; Riposan, I. Graphite degeneration in high Si, Mg-treated iron castings: Sulfur and oxygen addition effects. *Int. J. Met*. **2020**, *14*, 663–671.
9. Anca, D.; Chisamera, M.; Stan, S.; Stan, I.; Riposan, I. Sulfur and oxygen effects on high-Si ductile iron casting skin formation. *Coatings* **2020**, *10*, 618.
10. Anca, D.; Stan, I.; Chisamera, M.; Riposan, I.; Stan, S. Control of the Mg-treated iron casting skin formation by S-diffusion blocking at the metal—Mold interface. *Coatings* **2020**, *10*, 680.

11. Sofroni, L.; Ripoşan, I.; Brabie, V.; Chisamera, M. *Cast Iron*, EDP: Bucharest, Romania,1985.
12. Anca, D. Research on the Loss Modifyung Effect in the Superficial Layer Phenomenon of the Iron Castings. Ph.D. Thesis, Politehnica University of Bucharest, Bucharest, Romania, 2014.